Collector Receiver Design for Data Collection and Localization in Sensor-driven Networks

Bharath Ananthasubramaniam and Upamanyu Madhow

Abstract—We consider a sensor network in which the sensors communicate at will when they have something to report, without prior coordination with other sensors or with data collection nodes. The burden of demodulating the sensor data, and localizing the sensor which is communicating, falls on a network of collector nodes which are perpetually monitoring transmissions from the sensor network. This model allows the random deployment of very large numbers of sensor nodes with minimal capabilities, while shifting the complexity to a network of collector nodes. While the philosophy is similar to prior work on "imaging" sensor nets, the key difference is that the communication model is now sensor-driven, rather than collector-driven. The two major technical challenges addressed in this paper are as follows:

- (a) Are there simple physical layer implementations of the collector receiver for jointly solving the tasks of detection of a sensor transmission, estimation of the direction from which it comes, and demodulating the data?
- (b) Given that the collectors are not time synchronized well enough to permit the use of time-difference-of-arrival techniques for sensor localization, how well can the sensors be localized with spatial information alone, assuming that each collector node has a relatively small number of antennas?

The results reported in this paper indicate that the preceding issues can be addressed satisfactorily with appropriate design of the collector physical layer, together with Bayesian combining of the spatial information extracted by each collector.

I. INTRODUCTION

Sensor network deployments with tens of thousands of nodes are necessary to monitor large areas with the small sensing range of a typical microsensor. In such large networks, obtaining a prior map between a sensor's location and ID, which is often a critical part of the collected data, is difficult and sensor node functionality must be minimized to drive down the cost. To this end, we propose a sensor driven paradigm for data collection in large-scale sensor networks. Sensors transmit their data as soon as they observe an 'interesting' event, without prior coordination with the collectors or other sensors. A network of collectors that perpetually monitor for sensor transmissions are responsible for demodulating the sensor data, and localizing the transmitting sensor. Sensor node functionality is reduced by moving the complexity to the collectors, analogous to our prior work on imaging sensor nets[5].

In an imaging sensor net, a sophisticated collector scans the sensor field with a beacon. Sensors with data to send

This work was supported by the National Science Foundation under grants CCF-0431205, ANI-0220118, EIA-0080134 and CNS-0520335, and by the Office of Naval Research under grants N00014-03-1-0090 and N00014-06-1-0066

The authors are with the Department of Electrical and Computer Engineering, University of California, Santa Barbara, CA 93106, USA.

electronically reflect the beacon (thus creating a radar geometry) and modulate it with data, when illuminated by the collector. The collectors in such a *virtual radar* system create an "image" of the sensor field, which is a map between the sensor locations and the associated data, using radar and image processing techniques. Since the collector must initiate a sensor transmission, the data collection is *collector-driven* and differs from the on-demand *sensor-driven* communication. While the sensors can be localized using a single collector [4], multiple collectors can be used to increase localization accuracy.

The basic philosophy behind these two approaches are similar: the locations of the sensors are not known a priori (which is consistent with large-scale random deployments) and the sensors do not need to talk to each other, and the complexity is shifted to the collector nodes. Since a radar geometry is not induced by "at will" sensor transmissions, collaboration between multiple collector nodes is a must for sensor localization, rather than just being a performanceenhancing feature as in collector-driven imaging sensor nets. If the collector network has fine-grained time synchronization, then it is possible to use time-difference-of-arrival (TDoA) techniques to estimate the location of a transmitting sensor. However, such fine-grained synchronization is extremely difficult to achieve in a network of geographically dispersed collector nodes. In this paper, although we briefly indicate how localization can be achieved using spatial information alone, we focus on the physical layer design necessary for detection of a sensor transmission, estimation of the its direction of arrival, and demodulating the data.

An example of a sensor-driven network is the Remote Battlefield Sensor System (REMBASS) and its improvement (IREMBASS) [1] used by the US Department of Defence. These systems employ transmit-only sensor nodes for surveillance and situational awareness. However, the nodes are manually placed, so that there is a map between the node ID and its location. An architecture such as the one proposed here, which provides localization in sensor-driven systems, would allow random deployment of sensors on a much more massive scale than is currently possible in a system such as REMBASS or IREMBASS.

Our goal here is to design the collector receiver physical layer algorithms to realize such a sensor-driven system. Since there is no timing or phase-synchronization between the sensor and collectors, the collector receivers (each equipped with an antenna array) must, first, noncoherently accomplish joint detection and timing acquisition of the sensor transmission before demodulating the data and estimating

the AoA. Since the collectors perpetually monitor for sensor transmissions, the antenna array at the collector is connected to an automatic gain controller (AGC) to maintain the range of the input into the receiver RF circuitry within acceptable limits. A minimum mean-square error (MMSE) demodulator beamforms along the signal direction and produces the spatial correlation matrix for AoA estimation (seen in Figure 1). The acquisition algorithm is designed to acquire a single sensor transmission and we omit a discussion of multiple access interference between sensors that transmit in overlapping time intervals. While this can be handled by a combination of standard techniques such as spread spectrum modulation, space-time interference suppression at the collectors and delay randomization, the expected rate and spatial concentration (e.g., because of multiple neighboring sensors detecting a common event) of bursts of sensor transmissions must be accounted for. Using the angle of arrival (AoA) estimates of the sensor transmission from the above physical layer design, the collectors collaborate using a Bayesian algorithm to estimate the sensor location. Further, fundamental limits on the sensor localization performance and how the performance of the Bayesian localization scales with the number of collectors, the number of antennas per collector, and the signal-to-noise ratio (SNR) can be derived.

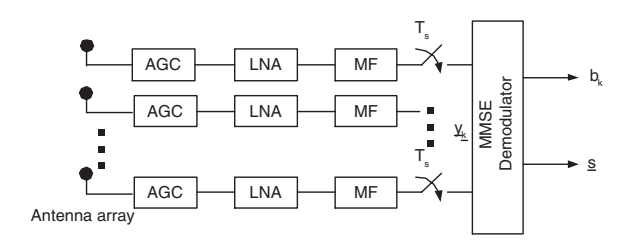


Fig. 1. RF frontend at each collector

Our main contributions are as follows. We motivate the choice of a MMSE demodulator and the mean-square error (MSE) as the detection statistic with an analysis of detection in the presence of an AGC. The linear MMSE demodulator and acquisition algorithm for joint detection and timing acquisition are described: The sensor begins its transmission with a training sequence, which is known to the collector to within a small bounded phase uncertainty. The collector hypothesizes on the possible phases of the current received bit, and runs one MMSE adaptation using the least-squares algorithm for each of them. If the minimum MSE is below a threshold, then the signal is declared 'detected' and the hypothesis corresponding to the minimum MSE is the estimated phase of the training sequence. After acquisition, the data is demodulated in a decision-directed fashion, constantly adapting the MMSE beamformer. The acquisition performance of the detector is studied using a combination of analysis and simulation.

Related Work: The receiver algorithms are based on prior work of one of the authors[15]. Since we are unaware of re-

lated work on receiver designs for sensor networks, we focus on literature related to the sensor-driven architecture. Emitter or source localization has been studied extensively for the last few decades for both defence and civilian applications[13]. Positioning using TDoA and it derivatives is used in cellular phone localization (as part of the E911 FCC mandate)[14], radar systems[23] and underwater acoustics[9]. In acoustic arrays, due to the lower speed of sound, timing synchronization (between collectors) required to get accurate localization using TDoA measurements can be obtained easily. This is utilized in [2] to localize an acoustic source using a collection of coarse microphones. However, at higher RF frequencies, timing synchronization to achieve localization of a few meters is difficult to achieve, as communication delays become significant sources of error. Acoustic localization with energy/signal strength measurements is presented using a method of projection onto convex sets in [7] and particle filtering in [22]. In [22], although Bayesian fusion of the sensor readings is employed, all the samples of the particle filter must be communicated between sensors leading to a high communication cost.

Signal strength indicators are unreliable at RF, as the path loss exponent and attenuation vary significantly with atmospheric conditions. Nevertheless, a combination of received signal strength, AoA and TDoA measured using RF radios are used in [8], [20], [16], [21] under a multi-hop setting for sensor self-localization with respect to a few known sensor locations or in a globally consistent coordinate framework. Triangulation-based techniques for sensor data fusion are discussed for TDoA estimates in [24], and for both TDoA and AoA measurements in [12]. A nonlinear least squares problem is solved for localization using acoustic AoA estimates in [6] and energy measurements in a distributed manner in [17]. In [3], maximum likelihood (ML) localization is formulated as a centralized two-dimensional search over the global likelihood function using both TDoA and AoA.

The rest of the paper is organized as follows. The analysis of detection in the presence of an AGC, the linear MMSE demodulator and the acquisition algorithm with its performance characterization is presented in Section II. The AoA estimation and Bayesian algorithm for sensor location is summarized in Section III. Concluding remarks are provided in Section IV.

II. COLLECTOR RECEIVER DESIGN

We first define the signal model for the collector receiver. In Section II-A, we present the analysis of the detection problem motivating the MMSE demodulator design. The detection performance is presented in Section II-D.

Each sensor uses BPSK modulation with energy per bit E_b to transmit its data. The effective transmit pulse seen at the receiver is p(t) of duration T. Each collector is equipped with an N-element uniform linear array (ULA) having a steering vector or array manifold, \underline{s}_{θ} , where θ is the baseband phase angle corresponding to an angle of arrival of arrival φ . The channel between each collector and the sensor

is line-of-sight (LOS) with additive white gaussian noise (AWGN). The complex proper gaussian noise (at baseband) has power N_0 per dimension. The local oscillators (LO) at the different collectors and the sensor are not mutually synchronized. The resulting random phase ϕ is assumed to be unknown and $U[-\pi,\pi]$, but remains constant throughout the sensor transmission. In addition, there is no symbol timing synchronization between the sensor and the collectors.

We model the AGC as a device that maintains the average power at its output at a constant level P_0 . In reality, the averaging interval of the AGC (to measure the input power) depends on its time constant or loop filter bandwidth. Nevertheless, this simple model captures most of the effects of the AGC. The baseband received signal at the antenna array of a collector prior to the AGC is

$$\underline{r}(t) = b(t - \tau) \underline{s}_{\theta} e^{j\phi} + \underline{n}(t),$$

where the transmitted bit stream is $b(t) = \sum_k b_k p(t-kT)$ and τ is the symbol timing error at the collector. Without loss of generality, τ is assumed to be in [0,T] and random phase $e^{j\phi}$ can be absorbed into the array manifold. Since the demodulator and the AoA estimator use the spatial correlation matrix, which is independent of the random phase, it is sufficient to use the equivalent coherent model,

$$\underline{r}(t) = b(t - \tau) \ \underline{s}_{\theta} + \underline{n}(t). \tag{1}$$

The signal at the output of the AGC is

$$\underline{y}(t) = \frac{\sqrt{P_0}}{\sqrt{E_b + N_0}} \left\{ \sum_k b_k \ p(t - kT - \tau) \ \underline{s}_{\theta} + \underline{n}(t) \right\},$$
(2)

where pulse energy ||p(t)|| = 1, and energy per bit $E_b = |b_k|^2 \ \forall k$. The output of the AGC (2) is passed through a symbol matched filter $p^*(-t)$ and sampled at the symbol rate T,

$$\underline{y}_n = \int_{rT}^{(n+1)T} \underline{y}(t) p(t - nT) dt. \tag{3}$$

The discrete-time coherent model is given by

$$\underline{y}_n = \sqrt{\alpha_{AGC}} \left\{ \underline{s}_{\theta} \{ b_n \lambda + b_{n-1} (1 - \lambda) \} + \underline{w}_n \right\}$$
 (4)

where $\lambda = \int_0^T p(t-\tau)p(t)dt$, $\alpha_{\rm AGC} = \frac{P_0}{E_b+N_0}$ and \underline{w} is an $N\times 1$ zero-mean complex circularly-symmetric AWGN vector with power N_0 per dimension. From (4), it is clear that there is inter-symbol interference due to the symbol timing error τ . Furthermore, the energy in b_k is split between \underline{y}_k and \underline{y}_{k+1} . Hence, both timing estimation and beamforming are essential to detect and demodulate the sensor transmission.

A. Detection in the presence of AGC

We now motivate our choice of an MMSE demodulator by presenting an analysis of detection in the presence of an AGC assuming that there is no symbol timing error. We model the two hypotheses, the presence and absence of a signal, as

$$H_1: \underline{y}_k = \sqrt{\alpha_{AGC}}(\underline{s}_{\theta}b_k + \underline{w}_k)$$
 (5)

$$H_0: \underline{y}_k = \sqrt{\frac{P_0}{N_0}}\underline{w}_k. \tag{6}$$

Under this model, the distributions of the output under the two hypothesis are

$$p(y|H_1) \sim CN(\sqrt{\alpha_{AGC}}\underline{s}_{\theta}b_k, \alpha_{AGC}N_0I_N)$$

 $p(y|H_0) \sim CN(0, P_0I_N)$

where I_n is an $n \times n$ identity matrix, and $CN(\underline{\mu}, \Sigma)$ stands for the proper complex Gaussian distribution with mean μ and covariance matrix Σ . Due to the lack of the priors for the detection, we declare hypothesis H_1 true if the ratio of $p(\underline{y}|H_1)$ and $p(\underline{y}|H_0)$ exceeds some threshold α . Eliminating the terms independent of \underline{y} , this ratio of $p(\underline{y}|H_1)$ and $p(\underline{y}|H_0)$ can be reduced to

$$||\underline{y} - \sqrt{\alpha_{\text{AGC}}}\underline{s}_{\theta}b||^2 \stackrel{1}{\leq} \alpha'. \tag{7}$$

Equation (7) suggests that the quality of fit (or squared error) of the received signal \underline{y} to the effective transmitted signal, $\sqrt{\alpha_{\text{AGC}}}\underline{s}_{\theta}b$, be compared with a threshold. However, \underline{s}_{θ} and b_k are not known a priori at the collector, and best choices for \underline{s}_{θ} and b_k are those that *minimize* this squared error. In order to maintain the squared error structure of the detection rule, we design an MMSE beamformer for the model in (4) to jointly estimate \underline{s}_{θ} and demodulate the data.

B. MMSE Demodulator

The linear MMSE demodulator for the asynchronous model in (4) to estimate the transmitted bit is given by

$$\hat{b}_n = \operatorname{sgn}(\langle \underline{c}_1, \underline{y}_n \rangle + \langle \underline{c}_2, \underline{y}_{n+1} \rangle) = \operatorname{sgn}(\langle \mathbf{c}, \mathbf{y}_n \rangle), \quad (8)$$

where \langle,\rangle denotes the standard inner product in Euclidean space, $\mathbf{c} = [\underline{c}_1^T \underline{c}_2^T]^T$, $\mathbf{y}_n = [\underline{y}_n^T \ \underline{y}_{n+1}^T]^T$ and the correlator \mathbf{c} minimizes the mean squared error $E\{|\langle\mathbf{c},\mathbf{y}_n\rangle-b_n|^2\}$. Note, the scaling factor $\sqrt{\alpha_{\mathrm{AGC}}}$ can be disregarded, since the demodulator in (8) is scale-invariant. Furthermore, the demodulator recovers all the energy in b_n by using both \underline{y}_n and y_{n+1} . The MMSE correlator is

$$\mathbf{c}_{\mathsf{MMSF}} = \mathbf{\bar{R}}^{-1} \tilde{\mathbf{u}}.$$

where $\bar{\mathbf{R}} = E[\mathbf{y}_n \mathbf{y}_n^H]$ is the spatial correlation matrix for the augmented system and $\tilde{\mathbf{u}} = E[b_n \mathbf{y}_n]$ is the correlation between the desired bit and the observed vector. The demodulator finds beamforming vectors \underline{c}_1 and \underline{c}_2 as complex scalar multiples closest to \underline{s}_{θ}^H in the MMSE sense. The MSE achieved by the MMSE solution is

$$\eta = 1 - \tilde{\mathbf{u}}^H \bar{\mathbf{R}}^{-1} \tilde{\mathbf{u}} = 1 - \mathbf{c}_{\text{MMSE}}^H \tilde{\mathbf{u}}, \tag{9}$$

setting $E_b=1$ without any loss of generality. In this paper, the MMSE solution is obtained by adaptation with respect to a known sequence b_n using a least-squares algorithm [11] (the choice of which will become clear in the discussion of the acquisition algorithm) followed by decision-direction demodulation using \hat{b}_n .

C. Acquisition Algorithm

We present an acquisition algorithm to jointly detect a sensor transmission and train the MMSE beamformer to demodulate the data. The collectors always suppose that there is a sensor transmission and attempt to receive it. A successful reception of a signal involves detecting the presence of the signal, and thereafter, acquiring the correct phase of the training sequence to obtain the symbol timing. During the acquisition phase, the sensor transmits a periodic training sequence t_n known to the collectors except for an unknown bounded phase uncertainty. Suppose t_n is a sequence of length M and period P. Hence, at each collector, the current bit $b_n = t_{n+i^*}$, where $i^* \in \{0, 1, \ldots, P-1\}$, but the corresponding i^* is unknown. Therefore, each collector runs P adaptive algorithms, each corresponding to a hypothesis H_i that the phase of the training is $i^* = i$, i.e.,

$$H_i: b_n = t_{n+i}, \quad i = 0, \dots, P-1.$$

The MMSE solution for *i*th hypothesis is $\mathbf{c}_i = \bar{\mathbf{R}}^{-1}\tilde{\mathbf{u}}_i$ where $\tilde{\mathbf{u}}_i = E\{t_{n+i}\mathbf{y}_n\}$. Note, that the augmented spatial correlation matrix $\bar{\mathbf{R}}$ needs to be computed and inverted only once every sample, and is common to all P adaptive algorithms. This reduces the computational burden of running P algorithms significantly.

When t_n is an random uncorrelated bit sequence, the autocorrelation of the periodic sequence is a Kronecker delta. For such a t_n , the MSE for the true hypothesis say i^* would be zero and MSE for all the other hypotheses is 1. Therefore, we choose good sequences with autocorrelation close to a Kronecker delta like a pseudonoise (PN) or Barker sequence. For the rest of the paper, we use a training sequence that is a repeated PN or Barker sequence of length P. A detailed discussion of the choice of good training sequences and their performance is beyond the scope of this paper (see [19]).

The acquisition algorithm has following steps: Step 1 (MMSE Solution Computation): Compute the MMSE beamformer and MSE for each hypothesis H_i as

$$\mathbf{c}_i = \bar{\mathbf{R}}^{-1} \tilde{\mathbf{u}}_i \quad \text{and} \quad \eta_i = \mathbf{c}_i^H \tilde{\mathbf{u}}_i.$$
 (10)

Step 2 (Finding the best hypothesis): Find the hypothesis $H_{i\min}$ with the minimum MSE, i.e.,

$$i_{\min} = \arg\min_i \eta_i.$$

Step 3 (Detection and Acquisition): For detection (during the training phase), compare $\eta_{i\min}$ against the detection threshold T. If $\eta_{i\min} < T$, then declare detected sensor transmission and correct phase of the training sequence as i_{\min} . Step 4 (Demodulation): After acquisition, the data is demodulated according to

$$\hat{b}_n = \operatorname{sgn}(\mathbf{c}_{i\min}^H \mathbf{y}_n).$$

The dimensionality of the adaptive algorithms is 2N, which is not very large as the number of antennas N typically takes values 2-8, and, as indicated earlier, the inverted correlation matrix is shared by the P parallel algorithms. Since the collectors need to detect a relatively short sensor

transmission, speed of convergence of the adaptive algorithms is most important. Therefore, we use a least-squares algorithm for acquisition that is faster and more complex, but the penalty for the added complexity is minimal for such small dimensional algorithms.

For the least-squares adaptation in Step 1, $\bar{\mathbf{R}}$ and $\tilde{\mathbf{u}}_i$ are replaced by empirical averages,

$$\hat{\mathbf{R}} = \frac{1}{M} \sum_{k=1}^{M} \mathbf{y}_k \mathbf{y}_k^H \quad \text{and} \quad \hat{\mathbf{u}}_i = \frac{1}{M} \sum_{k=1}^{M} t_{k+i} \mathbf{y}_k. \tag{11}$$

The corresponding correlator and MSE estimates, denoted by $\hat{\mathbf{c}}_i$ and $\hat{\mathbf{u}}_i$, are computed according to (10) using the empirical estimates in (11) and used in steps 2, 3 and 4 of the acquisition algorithm.

D. Detection Performance

We now discuss the selection of the detection threshold used in Step 3 of the acquisition algorithm. During operation of the receiver two events can occur: a correct detection, when the MSE due to the presence of a signal is below the threshold (we work with its complementary event a miss), or a false-alarm, when noise causes the MSE to go below the threshold. We denote the corresponding event probabilities by p_{miss} and p_{fa} respectively. There is a tradeoff between these two probabilities as increasing the threshold decreases p_{miss} and increases p_{fa} and vice-versa, when the threshold is decreased. We present this trade-off as a plot between p_{miss} and p_{fa} , which is called the receiver operating characteristics (ROC). In practice, the threshold and operating parameters like the threshold and length of training sequence M are chosen depending on the desired operating point on the tradeoff curve. The correlations introduced by inter-symbol interference makes the analysis of the p_{miss} for a given threshold challenging and it is left for ongoing work. Therefore, here we empirically estimate p_{miss} via simulations.

In the absence of a signal, the received signal is AWGN with power P_0 , independent of the absolute noise power N_0 (see (6)) due to the AGC. This ensures that for a given choice of threshold, the p_{fa} or rate of false alarms does not vary with changes in the background clutter and noise powers. Hence, this MMSE acquisition algorithm achieves a constant false alarm rate (CFAR), which is a desirable attribute in radar systems as well. Under the no signal hypothesis, we model the estimated MMSE solutions for the P training hypotheses as random correlators, i.e.,

$$\hat{\mathbf{c}}_i = \hat{\mathbf{R}}^{-1} \hat{\mathbf{u}}_i \approx \frac{1}{P_0} \hat{\mathbf{u}}_i = \frac{1}{MP_0} \sum_{k=1}^M t_{k+i} \mathbf{w}_k,$$

replacing $\hat{\mathbf{R}}$ by its mean P_0I_{2N} . Assuming the \mathbf{w}_k to be independent, the MMSE solutions are $\hat{\mathbf{c}}_i \sim CN(0, (P_0M)^{-1}I_{2N})$. The MSE for *i*th hypothesis is

$$\hat{\eta}_i = 1 - \hat{\mathbf{c}}_i^H \hat{\mathbf{u}}_i = 1 - \gamma_i,$$

where the random variables γ_i are gamma-distributed, $\gamma \sim \Gamma(2N,1/M)$, since it is the squared-norm of a complex proper Gaussian random vector with independent identically

distributed elements. Note, the gamma distribution is independent of the absolute signal or noise powers. Therefore, for a threshold T the false-alarm probability is given by

$$p_{fa} = P(\hat{\eta}_{i_{\min}} < T) = 1 - P(\hat{\eta}_{i} > T, i = 1, ..., P)$$
$$= 1 - P(\gamma < 1 - T)^{P}$$
(12)

For successful acquisition, the signal must be detected and the correct phase of the training sequence must be estimated. Simulations (not shown here) reveal that given successful detection, the probability of an incorrect phase estimate is extremely low. Therefore, we focus on the detection performance of the receiver alone. We simulate a collector receiver with N=2 antennas running P=7 parallel MMSE adaptations. The sensor transmits a P=7 length

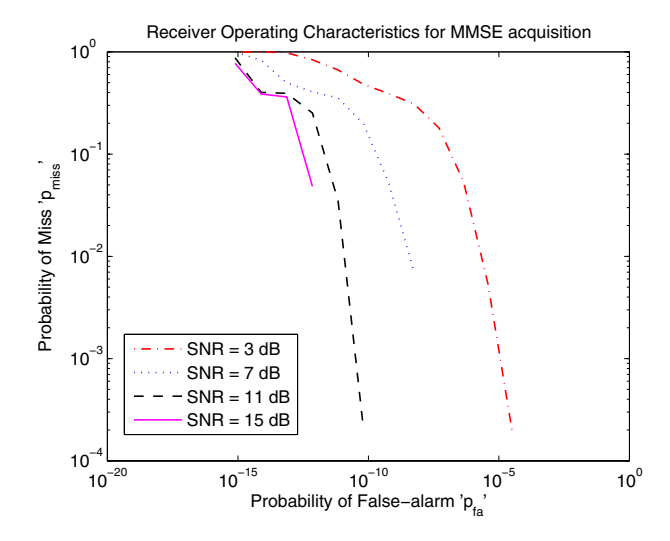


Fig. 2. The ROC: p_{miss} versus p_{fa} for a collector with 2 antennas using M=49 length training sequence running P=7 parallel adaptations at different SNRs

Barker sequence, which is repeated to form a M=49 length training sequence. In Figure 2, the ROC for this receiver is shown for different choices of SNR = E_b/N_0 . For each SNR, the p_{miss} was obtained from Monte-Carlo simulations and the corresponding p_{fa} is given by (12). It can be seen that p_{miss} improves monotonically with SNR for a given p_{fa} , since this receiver achieves CFAR. Therefore, it suffices to choose the threshold for the worst SNR expected and the performance will exceed the design criterion for higher SNRs. Suppose it is desired to operate such that $p_{miss} < p_1$ and $p_{fa} < p_2$, and the worst expected SNR is SNR₀. If from the ROC it is seen that (p_1, p_2) is not achievable at SNR₀ (the point is not in the region enclosed by the curve), then the length of training sequence M is increased until the desired performance can be achieved. Finally, when M and the desired operating point on the curve are found, the threshold corresponding to that p_{fa} is set using (12).

III. LOCALIZATION USING ANGLE OF ARRIVAL

We now summarize the Bayesian algorithm for sensor localization and provide a scaling law for the localization error. After acquiring the sensor transmission, the MMSE

demodulator is used to recover the transmitted data and estimate the AoA. The spatial (AoA) information in the sensor transmission is entirely captured in the estimated spatial correlation matrix $\hat{\mathbf{R}}$, which is computed as part of the acquisition algorithm. Furthermore, the $N \times N$ sub-block formed by the first N rows and columns of $\hat{\mathbf{R}}$ is sufficient (recall we used an augmented matrix), and this sub-matrix is denoted by R. The steering vector of the ULA at each collector is of the form $\underline{s}_{\theta} = [1 \ e^{j\theta} \ e^{j2\theta} \ \dots e^{j(N-1)\theta}]^T$, where $\theta = \frac{2\pi d \sin(\varphi)}{\lambda}$ and the AoA φ is the angle between the arriving plane wave and the plane of the array. The structure of \underline{s}_{θ} can used to accurately estimate the AoA using the root-MUSIC algorithm[10]. This algorithm finds the steering vector with the largest projection along the strongest eigenmode of R, and efficiently computes the AoA by finding the roots of an algebraic equation. However, in addition to the AoA estimate, the variance of the estimation error is also needed for the Bayesian algorithm. From empirical observations, the errors in the AoA are modeled as zero-mean Gaussian random variables with approximate variance[18] given by

$$\Sigma_{\varphi\varphi} \approx \frac{1}{N^3 M \text{SNR}},$$
 (13)

where M is the length of the training sequence used to estimate R. The AoA estimates from all the collectors must now be combined to estimate the sensor location. We assume that the localization errors along x- and y-axes are jointly Gaussian, so that all the probabilistic information can be captured by just tracking location estimates and their error covariances. The algorithm is initiated by the bootstrap procedure, in which the AoA from the first two collectors (according to some predefined ordering), are combined to compute an initial sensor location estimate and the variances of the estimation errors along the x- and y-axes. This estimate and error variances are passed as priors to the next collector that, after suitable coordinate transformations, updates the location estimate and error variances using its own AoA estimate. This simple procedure is repeated until all the available spatial information is incorporated into the location estimate. Since only a pair of mean and covariance estimates need to be passed on from one collector to the next, this algorithm can be implemented in a completely distributed manner, with each collector needing to know only its own location and orientation. While we consider AoA estimates here, the Bayesian algorithm is quite general, and can, for example, incorporate probabilistic information on the sensor range obtained from signal strength measurements.

To study the scaling of the localization performance with system parameters, we derive an estimate of the localization error in a circular sensor field using N_{coll} collectors, each equipped with N-element ULAs, spaced equally apart along the perimeter of the field. Using (13), a bound on the standard deviation of the localization error is given by

$$\sigma_s \le \frac{2}{\sqrt{N_{coll}} \cdot N^{\frac{3}{2}} \cdot \sqrt{MSNR}}.$$
 (14)

Equation (14) implies that an increase in the number of antenna elements per collector produces a cubic improvement

in performance as the number of collectors N_{coll} , length of the training sequence M and the SNR. The additional gain is due to beamforming (SNR gain) and narrower beam-patterns producing better AoA estimates (see (13)). Also, increasing N_{coll} and M improves performance at the same rate as SNR, since both parameters effectively provide better noise averaging. In Figure 3, the RMS localization of sensors in a circular field with unit radius obtained via simulations is shown, where each collector has 2 antennas. It is observed that good resolution can be obtained using spatial information alone and (14) accurately predicts the observed localization error.

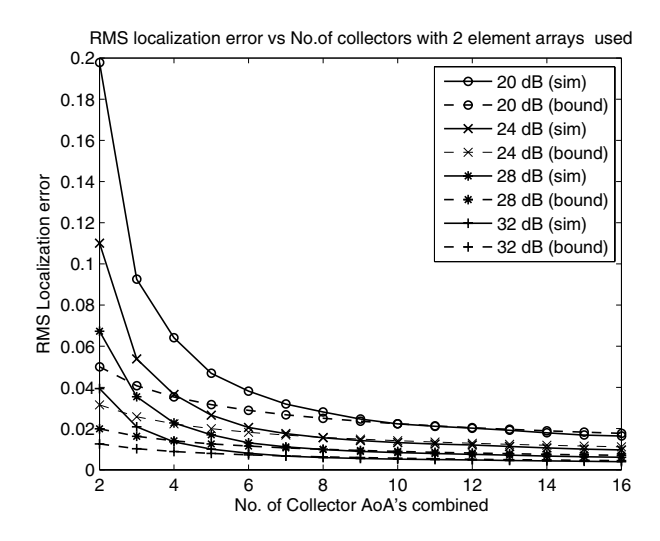


Fig. 3. Effect of No. of Collectors on localization: RMS localization error versus N_{coll} at different SNR_{eff} = M.SNR for N=2 element arrays. The corresponding analytic bounds are plotted with dotted lines.

IV. CONCLUSIONS

We designed a simple collector receiver to realize largescale randomly deployed sensor networks with sensor-driven data collection: sensor locations need not be known *a priori*, sensors can transmit at will without any coordination with each other or with the collectors, and collectors need not be time-synchronized. A linear adaptive MMSE receiver was used for detection, timing-acquisition and demodulation of the sensor transmission. The scale-invariant MSE is used as a detection criterion. The detection performance and the choice of operating point for the receiver were also presented. Our results indicate that fast joint detection and timing acquisition can be achieved with this receiver at moderate complexity.

The MMSE receiver also computes the spatial correlation matrix used for AoA estimation. We summarized the distributed Bayesian algorithm used to combine the different collector AoA estimates to localize the transmitting sensor. The dependence of the localization error on system parameters is also provided. Issues for future research include the effect of more realistic path loss models, methods for handling intersensor interference, utilizing additional information such as signal strength, understanding the effect of collector placements, and collaborative data demodulation and detection by the collectors with communication constraints.

REFERENCES

- "AN/GSQ-187 remote battlefield sensor system (REMBASS)." Military Analysis Network, Federation of American scientists, Feb 2000, http://www.fas.org/man/dod-101/sys/land/rembass.htm.
- [2] T. Ajdler, I. Kozintsev, R. Lienhart, and M. Vetterli, "Acoustic source localization in distributed sensor networks," in *Asilomar Conference* on Signals, Systems and Computers, vol. 3, Nov 2004, pp. 1328–1332.
- [3] A. Amar and A. Weiss, "Direct position determination of multiple radio signals," in *Proc. of ICASSP'04*, vol. 2, May 2004, pp. 17–21.
- [4] B. Ananthasubramaniam and U. Madhow, "Virtual radar approach to event localization in sensor networks," in *Proceedings of the International Symposium on Information Theory(ISIT 2004)*, Chicago, IL, June 2004, p. 517.
- [5] —, "Virtual radar imaging for sensor networks," in *Proceedings of the third international symposium on Information processing in sensor networks*. Berkeley, California, USA: ACM Press, New York, April 2004, pp. 294–300.
- [6] P. Bergamo, S. Asgari, H. Wang, D. Maniezzo, L. Yip, R. Hudson, K. Yao, and D. Estrin, "Collaborative sensor networking towards realtime acoustical beamforming in free-space and limited reverberance," *IEEE Trans. on Mobile Computing*, vol. 2, no. 3, pp. 211–224, July 2004
- [7] D. Blatt and A. Hero III, "Energy-based sensor network source localization via projection onto convex sets," *IEEE Trans. on Signal Processing*, vol. 54, no. 9, pp. 3614–3619, 2006.
- [8] N. Bulusu, J. Heidemann, D. Estrin, and T. Tran, "Self-configuring localization systems: Design and experimental evaluation," ACM Trans. on Embedded Computing Systems, vol. 3, no. 1, pp. 24–60, 2004.
- [9] G. Carter, Ed., Coherence and Time Delay Estimation. IEEE Press, 1993.
- [10] L. C. Godara, "Application of antenna arrays to mobile communications. ii. beam-forming and direction-of-arrival considerations," *Proc.* of *IEEE*, vol. 85, no. 8, pp. 1195–1245, Aug 1997.
- [11] S. Haykin, Adaptive Filter Theory, 3rd ed. Prentice Hall, 1996.
- [12] R. Kozick and B. Sadler, "Source localization with distributed sensor arrays and partial spatial coherence," *IEEE Trans. on Signal Process*ing, vol. 52, no. 3, pp. 601–616, March 2004.
- [13] H. Krim and M. Viberg, "Two decades of array signal processing research," *IEEE Signal Processing Magazine*, vol. 13, no. 4, pp. 67– 94, July 1996.
- [14] J. Liberti and T. Rappaport, Smart Antennas for Wireless Communication: IS-95 and Third Generation CDMA Applications. Prentice Hall, 1999.
- [15] U. Madhow, "MMSE interference suppression for timing acquisition and demodulation in direct-sequence CDMA systems," *IEEE Trans.* on Comm., vol. 46, no. 8, pp. 1065–1075, Aug 1998.
- [16] N. Priyantha, H. Balakrishnan, E. Demaine, and S. Teller, "Anchor-free distributed localization in sensor networks," MIT LCS, Tech. Rep. TR-892. Apr. 2003.
- [17] M. Rabbat, R. Nowak, and J. Bucklew, "Robust decentralized source localization via averaging," in *Proc. ICASSP'05*, vol. 5, Mar 2005.
- [18] B. Rao and K. Hari, "Performance analysis of root-music," *IEEE Trans. on Signal Processing*, vol. 37, no. 12, pp. 1939–1949, Dec 1989.
- [19] D. V. Sarwate, "Bounds on crosscorrelation and autocorrelation of sequences," *IEEE Trans. Inform. Theory*, vol. 25, pp. 720–724, Nov 1070
- [20] A. Savvides, H. Park, and M. Srivastava, "The bits and flops of the n-hop multilateration primitive for node localization problems," in *Proc. First ACM International Workshop on Wireless Sensor Networks and Application*, Atlanta, GA, Sept 2002, pp. 112–121.
- [21] Y. Shang and W. Ruml, "Improved MDS-based localization," in *Proc. of INFOCOM'04*, vol. 4, Mar 2004, pp. 2640–2651.
- [22] X. Sheng and Y. H. Hu, "Sequential acoustic energy based source localization using particle filter in a distributed sensor network," *IEEE Trans. on Signal Processing*, vol. 53, no. 1, pp. 44–53, Jan 2005.
- [23] M. Skolnik, Introduction to Radar Systems, 3rd ed. McGraw-Hill, 2000.
- [24] M. Wax and T. Kailath, "Optimum localization of multiple sources by passive arrays," *IEEE Trans. on Signal Processing*, vol. 31, no. 5, pp. 1210–1217, Oct 1983.